IEEE Access
Multidisciplinary | Rapid Review | Open Access Journal

Received January 29, 2021, accepted February 12, 2021, date of publication February 23, 2021, date of current version March 5, 2021.

Digital Object Identifier 10.1109/ACCESS.2021.3061529

Turbulent Flow of Water-Based Optimization Using New Objective Function for Parameter Extraction of Six Photovoltaic Models

DIAA SALAMA ABDELMINAAM[1,2], MOKHTAR SAID[3], AND ESSAM H. HOUSSEIN[4]

[1]Faculty of Computers and Artificial Intelligence, Benha University, Benha 12311, Egypt
[2]Faculty of Computer Science, Misr International University, Cairo 19648, Egypt
[3]Electrical Engineering Department, Faculty of Engineering, Fayoum University, Fayoum 63514, Egypt
[4]Faculty of Computers and Information, Minia University, Minia 61519, Egypt

Corresponding author: Diaa Salama Abdelminaam (diaa.salama@fci.bu.edu.eg)

This work was supported by the Misr International University, under Grant DSA28211231302952.

ABSTRACT With the development of new energy power systems, the estimation of the parameters of photovoltaic (PV) models has become increasingly important. Weather changes are random; therefore, the changes in the PV output power are periodic and nonlinear. Traditional power prediction methods are based on linearity, and relying only on a time series is not feasible. Consequently, metaheuristic algorithms have received considerable attention to extract the parameters of solar cell models and achieve excellent performance. In this study, the Turbulent Flow of Water-based Optimization (TFWO) is used to estimate the parameters of three traditional solar cell models, namely, Single-Diode Solar Cell Model (SDSCM), Double-Diode Solar Cell Model (DDSCM), and Three-Diode Solar Cell Model (TDSCM), in addition to three modified solar cell models, namely, modified SDSCM (MSDSCM), modified DDSCM (MDDSCM), and modified TDSCM (MTDSCM). Moreover, a polynomial equation of five degrees for the sum of squared errors (PE5DSSE) between the measured and calculated currents was used as a new objective function for extracting the parameters of the solar cell models. The proposed objective function delivered improved prediction accuracy than common objective functions. Experimental results revealed the effectiveness of TFWO compared with six counterparts, namely, ''Tunicate Swarm Algorithm (TSA), Grey wolf optimizer (GWO), modified particle swarm optimization (MPSO), Cuckoo Search algorithm (CSA), Moth flame optimizer (MFO) and Teaching Learning based optimization algorithm (TLBO),) for all the traditional and modified solar cell models based on the optimal parameters extracted using best PE5DSSE values.

INDEX TERMS Turbulent flow of water optimization (TFWO), metaheuristic algorithms (MHs), photovoltaic models, single diode solar cell model (SDSCM), double diode solar cell model (DDSCM), three diode solar cell model (TDSCM).

ABBREVIATIONS

PV	Photovoltaic
SDSCM	Single Diode Solar Cell Model
DDSCM	Double Diode Solar Cell Model
TDSCM	Three diode Solar Cell Model
MSDSCM	Modified Single Diode Solar Cell Model
MDDSCM	Modified Double Diode Solar Cell Model
MTDSCM	Modified Three Diode Solar Cell Model
TFWO	Turbulent Flow of Water Optimization
MPSO	Modified Particle Swarm Optimization
GWO	Grey Wolf Optimizer
CSA	Cuckoo Search Algorithm
TSA	Tunicate Swarm Algorithm
MFO	Moth Flame Optimizer
TLBO	Teaching Learning Based Optimization

The associate editor coordinating the review of this manuscript and approving it for publication was Valentina E. Balas.

I. INTRODUCTION

Human activities release excess carbon dioxide and other global warming gases into the atmosphere. Such gases act like a cover and trap heat in the atmosphere, resulting in significant and destructive impacts, including frequent storms and dry spells, rise in sea levels, and termination of animals [1].

Most renewable energy sources emit small to no global warming gases. Renewable energy obtained from biomass can produce a large number of global warming gases depending on the assets and whether the biomass is economically sourced and collected. Expanding the renewable energy supply can allow us to supplant carbon-intensive vitality sources and altogether decrease global warming emissions [2].

Solar energy is renewable. It is abundantly available, free, does not require transportation, and does not contaminate the environment. Sun-powered vitality facilitates a modern way of life for humankind and considers environment and ecological life into vitality preservation to diminish environmental contamination. It is the most common renewable source after wind energy [3]. Moreover, it is a promising vitality source that has expanded to incorporate numerous applications, including sun-powered water warming, sun-powered heating of buildings, sun-powered refining, sun-oriented pumping, sun-powered heaters, sun-oriented cooking, sun-powered electric control, sun-powered warm-control generation, and sun-powered greenhouses [4].

Solar energy is converted into a valuable power source using a photovoltaic (PV) model based on system based on the building block of the solar cell that converts light into electricity directly [5]. Solar PV innovation is considered a significant renewable energy source worldwide [6]. Recently, considerable financial enhancements within the PV control industry have been achieved, thus enabling a clean future for this innovation. PV can influence humans from all walks of life, such as mortgage holder, agriculturist, planner, architect, or electricity user. PV was first used in space programs. Currently, PV frameworks are used to produce power-to-pump water, illuminate the night sky, actuate switches, charge batteries, and supply electric utility lattice, among others.

An essential aspect of improving the efficiency of PV systems is determining an optimal design for the system. Therefore, a reliable and optimal PV system model must be established to improve the operating characteristics of the overall PV system [7]. The modeling process can be divided into two independent stages. The first stage involves the preparation of the mathematical model of the PV system, and the second stage involves the accurate parameter estimation technique for precise PV cell modeling and the analysis of PV system characteristics. However, the high nonlinearity of the output I–V curve makes the optimal design for the system very difficult. Many PV solar cell models describe the nonlinear performance of the solar PV system, such as The Single Diod PV (SDPV), a Double Diode PV (DDPV), and a Triple-Diode PV (TDPV) [8]

The SDPV model is the basic PV solar cell model and is the most popularly used model owing to its simplicity, smaller number of unidentified parameters, and higher accuracy. Therefore, the SDPV model exhibits a straightforward structure with fast dynamic behavior. The DDPV model achieves more accurate modeling of the PV panels than the SDPV model; further, the DDPV model shows losses in the P–N junction's quasineutral and space-charge regions [9]. The DDPV model has seven unknown parameters that must be estimated; therefore, it simulated as a mathematical model. In a study by Kaur *et al.* [10], the three-diode model is presented as a model with ten parameters that increase the exactness of the estimation process and make the PV cell model suitable for manufacturing applications. The TDPVis considered the best PV solar cell model, although its design is complicated. The consistent modeling of the PV system is a challenging task that typically depends on the formulation of the mathematical simulation model and the exact estimation of the unknown parameters [11].

Different approaches have been used to fine-tune the unknown parameters (maximum ten parameters) of the PV model. In recent literature, the SDPV, DDPV, and TDPV models of the PV modules have been widely investigated because of their unknown parameters determined using analytical techniques and metaheuristic (MH) optimization approaches [12].

Analytical techniques have been used to estimate the PV parameters using different selected points. The analytical approach is based on the derivation of mathematical equations that necessarily provide simple and rapid identification and calculation of the PV parameters. In analytical approaches, the main points of the I–V characteristic curves were used, namely, the point of the short circuit current, open-circuit voltage, and the maximum power. Despite the simplicity and short calculation time, the accuracy of analytical approaches can decrease if one or more critical points of the I–V characteristics are incorrectly determined [13]. Moreover, the analytical approach does not reflect the real operating conditions. Several analytical techniques have been reported in the literature [14].

The Lambert method is a strategy for predicting the obscure parameter values of the one- and two-diode modes of the sun-powered PV cells. This approach is less accurate than the numerical approaches. Numerical calculation strategies generally involve nonlinear calculations, such as the Newton–Raphson method [15], Nelder–Mead simplex strategy [16], conductivity strategy [17], and Levenberg–Marquardt (LM) calculation, to distinguish the parameters of the reenactment models of the PV framework [18]. In this setting, multiple numerical procedures are presented in a study [**?**]. In any case, notwithstanding the precision of the explanatory approaches, numerous obscure parameters within the numerical strategies complicate the extraction procedure.

A comprehensive survey on MH calculations and related variations [20]–[22] has been performed on the PV cell parameters. These calculations are primarily classified into four categories: biology-, physics-, sociology-, and mathematics-based calculations.

The primary category of MH calculations for PV cell modeling and parameter estimation is biology-based calculations, such as genetic algorithm (GA) and differential evolution (DE). In the same setting, the adaptive GA method can yield higher computation efficiency of parameter

estimation [23] than traditional GA methods. In the same context, the improved versions of DE [24],have been proposed to enhance the convergence speed and global search quality, such as artificial bee swarm optimization [25], artificial bee colony algorithm, teaching–learning-based artificial bee colony [26], whale optimization algorithm (WOA) [27], improved WOA [28], and chaotic WOA [29]. In addition to modified WOA, improved antlion optimizer [30], and biogeography-based optimization (BBO) [31], the BBO–M strategy incorporates the mutation strategy of DE into the original migration of BBO [31], to effectively enhance the exploitation capability and overcome the shortcomings of the conventional BBO, which can easily determine an optimum when the PV cell parameter identification is applied using the cuckoo search (CS) [32]. A hybrid version of CS, called biogeography-based heterogeneous CS algorithm, is proposed [33] to improve the accuracy and reliability of various algorithms, such as original CS, bird-mating optimization (BMO) [34], simplified BMO [35], Flower pollination algorithm (FPA) [**?**], hybrid bee pollinator FPA [36], Grey wolf optimization (GWO) [37], Bacterial foraging algorithm [38], Artificial immune system [39], and Salp swarm algorithm.

Simulated results show the significant superiority of MH algorithms for modeling model the PV cells based on the category of biology-based algorithms. Hence, such strategies can be considered robust and effective tools to solve the identification problem of PV cells.

The second category of MH calculations for PV cell modeling and parameter estimation is the physics-based calculation. This category incorporates calculations that are used for parameter identification, such as particle swarm optimization (PSO) (and its improved models [40],), parallel chaos optimization algorithm (PCOA), modified PCOA (MPCOA) [41], simulated annealing (SA) algorithm [42], hybrid method (LM+SA) [17], firework algorithm [43], wind-driven optimization [44], evaporation rate-based water cycle algorithm (an improved version of water cycle algorithm (WCA)), and improved Lozi map-based chaotic optimization algorithm [45]. All these physics-based algorithms have been used for identifying the parameters of PV cells.

The third category of MH algorithms PV cell modeling and parameter estimation is the sociology-based algorithms. This category includes algorithms that are used for parameter identification, such as harmony search (HS) algorithm, grouping-based global HS [46], (an improved variant of HS), teaching–learning-based optimization (TLBO) algorithm [47], improved and simplified TLBO (STLBO) algorithm [44], imperialist competitive algorithm (ICA) [44] and multiple learning backtracking search algorithm. Compared with GA and PSO, ICA has a higher convergence speed and accuracy and more substantial convergence stability, particularly for low-dimensional optimizations. Based on backtracking search algorithm [48], all sociology-based algorithms and approaches have been used for PV cell parameter identification for SDM and DDM.

The fourth category of MH calculations for PV cell modeling and parameter estimation is the mathematics-based calculation. This category incorporates calculations used for parameter estimation, such as pattern search algorithm [49], shuffled complex evolution algorithm [50] Jaya algorithm, and modified Jaya algorithm.

In summary, the major contributions of this study are as follows:

- The polynomial equation of five degrees for the sum of squared errors (PE5DSSE) between the measured and calculated currents is used as a new objective function for extracting parameters of the solar cell models.
- New MH algorithms and turbulent flow of water-based optimization (TFWO) are used for identifying the solar cell parameters.
- The performance of the proposed algorithm is compared with those of other algorithms, such as tunicate swarm algorithm (TSA), GWO, modified particle swarm optimization (MPSO), CS algorithm (CSA), moth flame optimizer (MFO), and TLBO algorithm.
- The parameters of traditional solar cell models, namely, single-diode solar cell model (SDSCM), double-diode solar cell model (DDSCM), and three-diode solar cell model (TDSCM), are estimated.
- The parameters of the modified solar cell models, namely, modified SDSCM (MSDSCM), modified DDSCM (MDDSCM), and modified TDSCM (MTDSCM), are estimated.
- The modified and traditional solar cell models are compared based on the new PE5DSSE value.
- The characteristic curves of SDSCM, DDSCM, TDSCM, MSDSCM, MDDSCM, and MTDSCM are simulated based on the optimal parameters extracted using the best PE5DSSE value from the TFWO algorithm.

The remainder of this paper organization is as follows. The analysis of photovoltaic models is presented in Section II. The new objective function is discussed in Section III. An overview of TFWO is shown in Section IV. The experimental results and discussion are presented in Section V. The conclusion of this paper is summarized in Section VI.

II. ANALYSIS OF PHOTOVOLTAIC MODELS

The traditional PV models, such as SDSCM, DDSCM, and TDSCM, and modified PV models (MSDSCM, MDDSCM, and MTDSCM) are analyzed in this section.

A. SINGLE DIODE SOLAR CELL MODEL (SDSCM)

Figure 1 shows the equivalent circuit of SDSCM. Based on this circuit, the current generated from SDSCM is determined using the following equation:

$$I = I_{ph} - I_{d1} - I_{sh} \tag{1}$$

$$I = I_{ph} - I_{o1}\left[e^{\frac{q(V+IR_s)}{n_1 KT_c}} - 1\right] - \frac{V + IR_s}{R_{sh}} \tag{2}$$

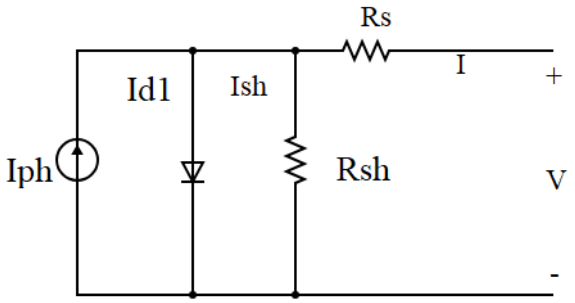

FIGURE 1. Single diode equivalent model.

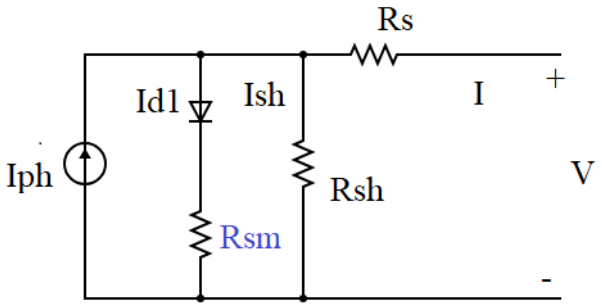

FIGURE 2. Modified single diode equivalent model.

where I; is the current output from SDSCM, I_{ph} is the photo generated current, the shunt current is I_{sh}, I_{d1} is the diode current, R_{sh} is the shunt resistance, R_s is the series resistance, n_1 is the diode ideality factor, K is Boltzmann's constant, q is the charge of electron, T_c is the cell temperature.

B. MODIFIED SINGLE DIODE SOLAR CELL MODEL (MSDSCM)

Figure 2 shows the equivalent circuit of MSDSCM. Based on this circuit, the current generated from MSDSCM is determined using the following equation:

$$I = I_{ph} - I_{o1}\left[e^{\frac{q(V+IR_s-I_{d1}R_{sm})}{n_1KT_c}} - 1\right] - \frac{V+IR_s}{R_{sh}} \quad (3)$$

The losses in the quasi-neutral region is expressed by adding the modified series resistance; R_{sm}.

C. DOUBLE DIODE SOLAR CELL MODEL (DDSCM)

Figure 3 shows the equivalent circuit of DDSCM. Based on this circuit, the current generated from DDSCM is determined using the following equation:

$$I = I_{ph} - I_{d1} - I_{d2} - I_{sh} \quad (4)$$

$$I = I_{ph} - I_{o1}\left[e^{\frac{q(V+IR_s)}{n_1KT_c}} - 1\right] - I_{o2}\left[e^{\frac{q(V+IR_s)}{n_2KT_c}} - 1\right] - \frac{V+IR_s}{R_{sh}} \quad (5)$$

where I_{d2} is the current in the second diode, n_2 is the ideality factor of the second diode.

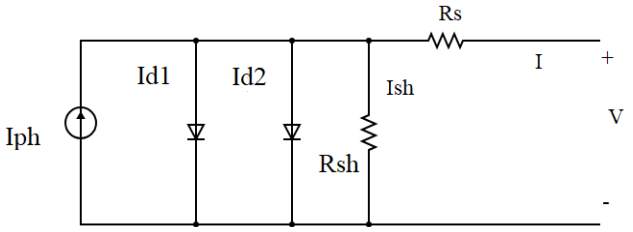

FIGURE 3. Double diode equivalent model.

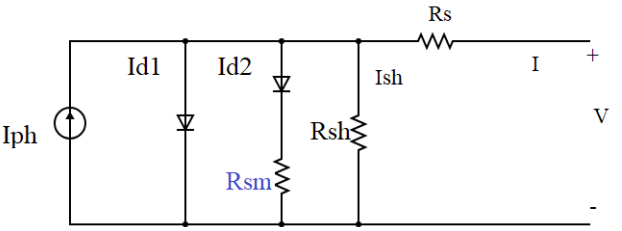

FIGURE 4. Modified double diode equivalent model.

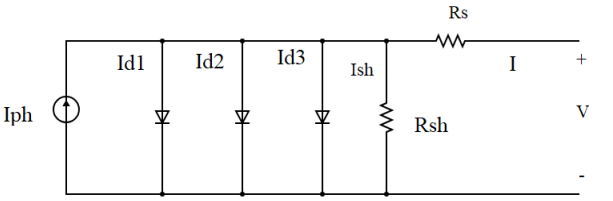

FIGURE 5. Three diode equivalent model.

D. MODIFIED DOUBLE DIODE SOLAR CELL MODEL (MDDSCM)

Figure 4 shows the equivalent circuit of MDDSCM. Based on this circuit, the current generated from MDDSCM is determined using the following equation.

$$I = I_{ph} - I_{o1}\left[e^{\frac{q(V+IR_s)}{n_1KT_c}} - 1\right] - I_{o2}\left[e^{\frac{q(V+IR_s-I_{d2}R_{sm})}{n_2KT_c}} - 1\right] - \frac{V+IR_s}{R_{sh}} \quad (6)$$

The losses in the space charge region is expressed by adding the modified series resistance; R_{sm} in the second diode.

E. THREE DIODE SOLAR CELL MODEL (TDSCM

Figure 5 shows the equivalent circuit of TDSCM. Based on this circuit; the current generated from TDSCM is determined using the following equation:

$$I = I_{ph} - I_{d1} - I_{d2} - I_{d3} - I_{sh} \quad (7)$$

$$I = I_{ph} - I_{o1}\left[e^{\frac{q(V+IR_s)}{n_1KT_c}} - 1\right] - I_{o2}\left[e^{\frac{q(V+IR_s)}{n_2KT_c}} - 1\right] - I_{o3}\left[e^{\frac{q(V+IR_s)}{n_3KT_c}} - 1\right] - \frac{V+IR_s}{R_{sh}} \quad (8)$$

where I_{d3} is the current in the third diode, n_3 is the ideality factor of the third diode.

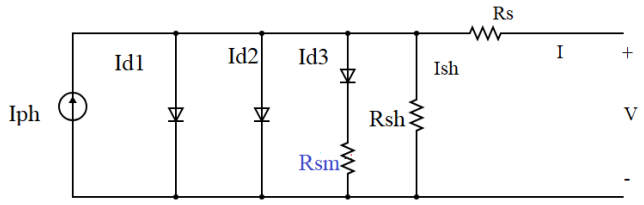

FIGURE 6. Modified three diode equivalent model.

F. MODIFIED THREE DIODE SOLAR CELL MODEL (MTDSCM)

Figure 6 shows the equivalent circuit of MTDSCM. Based on this circuit, the current generated from MTDSCM is determined using the following equation.

$$I = I_{ph} - I_{o1}\left[e^{\frac{q(V+IR_s)}{n_1KT_c}} - 1\right] - I_{o2}\left[e^{\frac{q(V+IR_s)}{n_2KT_c}} - 1\right] - I_{o3}\left[e^{\frac{q(V+IR_s-I_{d3}R_{sm})}{n_3KT_c}} - 1\right] - \frac{V+IR_s}{R_{sh}} \quad (9)$$

The losses in the defect region is expressed by adding the modified series resistance; R_{sm} in the third diode.

III. OBJECTIVE FUNCTION

To measure the consistency between the measured and simulated data, the PV models (SDSCM, MSDSCM, DDSCM, MDDSCM, TDSCM, and MTDSCM) were evaluated using a new objective function for estimating the parameters of each model. The new objective function is PE5DSSE between the measured and simulated current data. The mathematical equations for PE5DSSE are expressed as follows:

$$J\,(V.I.X) = I - I_{exp} \quad (10)$$

$$SSE = \sum_{1}^{N} J\,(V.I.X)^2 \quad (11)$$

$$PE5DSSE = SSE + SSE^2 + SSE^3 + SSE^4 + SSE^5 \quad (12)$$

where I_{exp}, is the measured current, N is the number data set and X is the variables required to estimate. The decision variable vector for SDSCM is:

$$X = (I_{ph}.\ I_{o1}.\ n.\ R_s \ \text{ and } \ R_{sh}).$$

The decision variable vector for DDSCM is:

$$X = (I_{ph}.\ I_{o1}.\ n.\ R_s.\ R_{sh}.\ I_{o2}\ and\ n_2).$$

The decision variable vector for TDSCM is:

$$X = (I_{ph}.\ I_{o1}.\ n_1.\ R_s.\ R_{sh}.\ I_{o2}.\ n_2.\ I_{o3} \ \text{ and } \ n_3).$$

The decision variable vector for MSDSCM is

$$X = (I_{ph}.\ I_{o1}.\ n_1.\ R_s.\ R_{sh} \ \text{ and } \ R_{sm}).$$

The decision variable vector for MDDSCM is:

$$X = (I_{ph}.\ I_{o1}.\ n.\ R_s.\ R_{sh}.\ I_{o2}.\ n_2 \text{ and } \ R_{sm}).$$

TABLE 1. The limits of estimated parameters [33].

Parameter	Lower bound	Upper bound
I_{ph}	0	1
$I_{o1}.\ I_{o2}\ and\ I_{o3}\ \ (\mu A)$	0	1
$R_s.R_{sm}$	0	0.5
R_{sh}	0	100
$n_1.n_2\ and\ n_3$	1	2

The decision variable vector for MTDSCM is:

$$X = (I_{ph}.\ I_{o1}.\ n_1.\ R_s.\ R_{sh}.\ I_{o2}.\ n_2.\ I_{o3}.\ n_3 \ \text{ and } \ R_{sm}).$$

The parameters for the SDSCM, DDSCM, TDSCM, MSDSCM, MDDSCM and MTDSCM are identified with the proposed TFWO algorithm for R.T.C France solar cell. The proposed algorithm TFWO results are compared with other algorithms such as Tunicate Swarm Algorithm (TSA) [51], Grey wolf optimizer (GWO) [52], modified particle swarm optimization (MPSO) algorithm [53], Cuckoo Search algorithm (CSA) [54], Moth flame optimizer (MFO) [55] and Teaching Learning based optimization algorithm (TLBO) [56]. the limit of estimated parameters [33] are shown in Table 1.

IV. TURBULENT FLOW OF WATER-BASED OPTIMIZATION (TFWO)

TFWO [57], is a recent MH algorithm. It is inspired by the whirlpool phenomenon created in a turbulent flow of water. A whirlpool moves in a circular motion along a tight route. The center of the whirlpool is a hole that sucks the particles around it toward the middle and then draws the particles inside the vortex. In the TFWO algorithm, the population is divided into NWh groups and the best member of each group is set in the center of the whirlpool.

a: FORMATION AND EFFECTS OF WHIRLPOOLS

The algorithm divides the initial population (x^0) and comprising N_p members set equally between the N_{Wh} whirlpool. Moreover, by applying a centripetal force on each whirlpool (Wh), and plunging them into its well, the positions of objects in a specific set (X) were integrated with its central position. Then, each whirlpool jth (with their local position on Wh_j, integrating the X_i object position with itself; this implies that (($X_i = Wh_j$). If this integration is not performed, some deviations (ΔX_i) will occur for other (Wh) whirlpools owing to the distance ($Wh - Wh_j$) between them and their objective values ($f()$). Therefore, the ith new position of the object will be equal to$X_i^{new} = Wh_j - \Delta X_i$. Moreover, around their whirlpool's center and approach, the motion of the objects (X) is restricted by the special angle (δ), which changes at each iteration as follows:

$$\delta_i^{\text{new}} = \delta_i + \text{rand}_1 \times \text{rand}_2 \times \pi \quad (13)$$

The angle ΔX_i has been calculated depending on the distance of the whirlpools from all the objects with the least and

most weights based on Eqs. 14 and 15 respectively. Then, the particle's position is updated from Eq. (16).

$$\Delta_t = f\left(Wh_t\right) \times \left|Wh_t - \text{sum}\left(X_i\right)\right|^{0.5} \tag{14}$$

$$\begin{aligned}\Delta X_i = &\left(\cos(\delta_i^{\text{new}}\right) \times \text{rand}\left(1,\text{D}\right) \times \left(Wh_f - X_i\right) \\ &- \sin\left(\delta_i^{\text{new}}\right) \times \text{rand}(1, D) \times \left(Wh_w - X_i\right)\Big) \\ &\times \left(1 + \left|\cos\left(\delta_i^{\text{new}}\right) - \sin\left(\delta_i^{\text{new}}\right)\right|\right)\end{aligned} \tag{15}$$

$$X_i^{\text{new}} = Wh_j - \Delta X_i \tag{16}$$

where the δ_i is the *ith* object's angle and the whirlpools with the minimum and maximum values of Δ_t are Wh_f and Wh_W, respectively.

A. THE MATHEMATICAL MODEL

This subsection presents an overview of the mathematical steps for the TFWO algorithm as follows:

1) *Updating object's position phase:* The updating of object's position is summarized in the following two steps:

Step 1:

for t = 1 N_{Wh}

$\Delta_t = f(Wh_t) \times |Wh_t - sum(X_i)|^{0.5}$

end

Wh_f=Wh_t with min value of Δ_t

Wh_w=Wh_t with max value of Δ_t

$\delta_i^{\text{new}} = \delta_i + \text{rand}_1 \times \text{rand}_2 \times \pi$

ΔX_i=$\left(\cos\left(\delta_i^{\text{new}}\right) \times \text{rand}\left(1, D\right) \times \left(Wh_f - X_i\right)\right.$

$\left. - \sin\left(\delta_i^{\text{new}}\right) \times \text{rand}(1, D) \times \left(Wh_w - X_i\right)\right)$

$\times \left(1 + \left|\cos\left(\delta_i^{\text{new}}\right) \times - \sin\left(\delta_i^{\text{new}}\right)\right|\right)$;

$X_i^{\text{new}} = Wh_j - \Delta X_i$;

Step 2:

$X_i^{\text{new}} = \min\left(\max\left(X_i^{\text{new}}, X^{\min}\right), X^{\max}\right)$;

if $f\left(X_i^{\text{new}}\right) <= f\left(X_i\right)$

$X_i = X_i^{\text{new}}$

$f\left(X_i\right) = f\left(X_i^{\text{new}}\right)$;

end

2) *Centrifugal force phase:*

From Newton's first law of motion, although the centripetal force FE_i pulls the moving objects toward their whirlpool, FEi occasionally overcomes the centripetal force of the whirlpool; therefore, the object randomly moves to a new position. Then, the centrifugal force moves them away from the corresponding center. Moreover, the centrifugal force and action use Eq.(17) and Eq. (18) respectively. Additionally, the mathematical model of the centrifugal force phase is summarized in Step 3.

$$FE_i = \left(\left(\cos\left(\delta_i^{\text{new}}\right)\right)^2 \times \left(\sin\left(\delta_i^{\text{new}}\right)\right)^2\right)^2 \tag{17}$$

$$x_{i,p} = x_p^{\min} + rand \times \left(x_p^{\max} - x_p^{\min}\right) \tag{18}$$

Step 3:

FE_i=$\left(\left(\cos\left(\delta_i^{\text{new}}\right)\right)^2 \times \left(\sin\left(\delta_i^{\text{new}}\right)\right)^2\right)^2$.

if rand $< FE_i$

$p = \text{round}(1 + \text{rand} \times (D - 1))$;

$x_{i,p} = x_p^{\min} + \text{rand} \times \left(x_p^{\max} - x_p^{\min}\right)$;

$f\left(X_i\right) = f\left(X_i^{\text{new}}\right)$;

end

3) *Interactions between the whirlpools phase:*

The effects of whirlpools on the objects have been modeled. Every whirlpool tends to unite its own position with that of the considered whirlpool, which is similar to the effects of a whirlpool on the surrounding objects. Therefore, the minimum amount of nearest whirlpool is calculated using Eq. (19) based on its objective function. To update the whirlpool position, Eqs. (20) and (21) are defined as follows.

$$\Delta_t = f(Wh_t) \times \left|Wh_t - sum(Wh_j)\right| \tag{19}$$

$$\begin{aligned}\Delta Wh_j = &\ rand(1, D) \times \left|cos(\delta_j^{new}) + sin(\delta_j^{new})\right| \\ &\times (Wh_f^{new} - Wh_j^{new})\end{aligned} \tag{20}$$

$$Wh_j^{new} = Wh_f - \Delta Wh_j \tag{21}$$

where, value of the j^{th} whirlpool hole's angle is acts by δ.

To summarize the above phenomenon, we use Steps 4 and 5, which illustrate the relation between the whirlpool interactions:

Step 4:

for t = 1: N_{Wh} − j

Δ_t = f(Wh_t) × $\left|Wh_t - sum(Wh_j)\right|$

end

Wh_f = Wh with min value of Δ_t

$Wh_j^{new} = Wh_f - \Delta Wh_j$;

$\Delta Wh_j = rand(1, D) \times \left|cos(\delta_j^{new}) + sin(\delta_j^{new})\right| \times (Wh_f^{new} - Wh_j^{new})$;

$\delta_j^{new} = \delta_j + rand_1 \times rand_2 \times \pi$.

Step 5:

Wh_j^{new} = min(max(Wh_j^{new},X^{min}), X^{max});

if f(Wh_j^{new}) ≤ f(Wh_j)

$Wh_j = Wh_j^{new}$;

f(Wh_j) = f(Wh_j^{new});

end

4) *The strongest member phase:*

Among the new members obtained for the whirlpool, the strongest member is selected for the next iteration according to the least value of the objective function compared with its corresponding whirlpool. To summarize this phase, Step 6 illustrates the selected new strongest whirlpool.

Step 6:

if f(X_{best}) ≤ f(Wh_j)

$Wh_j \leftrightarrow X_{best}$

end

V. RESULTS OF SOLAR CELL MODELS

The identified parameters of the traditional and improved solar cell models are established in this section using the R.T.C France solar cell. The proposed TFWO algorithm uses the estimated parameters. Several algorithms, such

TABLE 2. The parameters identified SDSCM at the best PE5DSSE.

Algorithm	I_{pv}(A)	I_{o1}(A)	n_1	$R_s(\Omega)$	$R_{sh}(\Omega)$	PE5DSSE
TFWO	0.760775531	3.23E-07	1.481183449	0.036377098	53.71847884	2.5278E-05
TSA	0.759651581	4.48E-07	1.514925671	0.034284154	59.17997317	1.0342E-04
GWO	0.761892916	2.62E-07	1.460549039	0.036930555	38.69585787	4.6607E-05
CSA	0.760768025	3.18E-07	1.479574211	0.036479634	54.33208432	2.55E-05
MFO	0.760801792	3.05E-07	1.475378613	0.036605708	52.18719053	2.56E-05
MPSO	0.760842092	1.00E-06	1.604529829	0.031385035	100	0.000155841
TLBO	0.760733138	3.28E-07	1.482619484	0.03632304	54.45018775	2.5308E-05

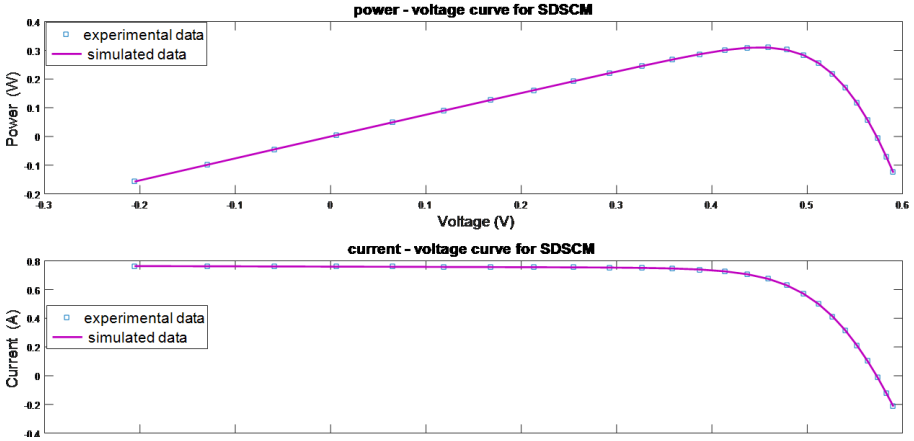

FIGURE 7. I-V and P-V curves for SDSCM at the best PE5DSSE from TFWO.

as TSA [51], Grey wolf optimizer (GWO) [52], modified particle swarm optimization (MPSO) algorithm [53], Cuckoo Search algorithm (CSA) [54], Moth flame optimizer (MFO) [55] and Teaching Learning based optimization algorithm (TLBO) [56], are compared with the proposed TFWO algorithm. The algorithms used in this study extract the solar cell parameters of each model based on the new objective function. TFWO and all compared algorithms were evaluated using 30 independent runs (with 1000 iterations in each run) and 30 search agents.

A. RESULTS OF THE TRADITIONAL SOLAR CELL MODELS

The results for the traditional solar cell models, namely, SDSCM, DDSCM, and TDSCM, are discussed in this subsection. The estimated parameters of these models are based on the new objective function. PE5DSSE in terms of the proposed TFWO algorithm and other compared algorithms is discussed. The I–V and P–V curves of the R.T.C France solar cell for SDSCM, DDSCM, and TDSCM are illustrated using the best PE5DSSE value for the proposed TFWO algorithm.

1) SDSCM RESULTS

The parameters extracted from the seven algorithms for SDSCM explain in table: 2. Based on this data the best value of PE5DSSE is 2.5278E-05, that is achieved by the TFWO algorithm, the TLBO algorithm achieve the second best PE5DSSE (2.5308E-05), then CSA, MFO, GWO, TSA and MPSO respectively. Figure 7 explains the I-V and P-V curves for SDSCM at the best value of PE5DSSE from the proposed TFWO. Figure 8 explains the absolute error for current and power curves for SDSCM at the best value of PE5DSSE from the proposed TFWO. Based on these figures; the maximum absolute error for current is 0.00250741232809032, the maximum absolute error for power is 0.00146257361097508.

TABLE 3. The parameters identified DDSCM at the best PE5DSSE.

Algorithm	TFWO	TSA	GWO	CSA	MFO	MPSO	TLBO
I_{ph} (A)	0.760782649	0.761596972	0.760344717	0.760605415	0.760775449	0.761455939	0.760790337
I_{o1} (A)	8.51E-07	6.39E-07	8.67E-07	2.73E-07	3.22E-07	1.00E-06	1.91E-07
n_1	2	1.822321387	1.819122901	1.465394638	1.480916755	1.613067165	1.439027715
R_s (Ω)	0.036798739	0.032755663	0.034638894	0.036687025	0.036381615	0.030003235	0.036809732
R_{sh} (Ω)	55.71595216	74.20164067	87.09346055	50.5726416	53.72789904	100	55.3835229
I_{o2} (A)	2.14E-07	4.38E-07	2.65E-07	1.04E-07	6.02E-09	1.00E-06	6.24E-07
n_2	1.446533118	1.526563335	1.480267595	1.938049485	2	2	1.870881842
PE5DSSE	2.51E-05	0.000133951	6.27E-05	2.88E-05	2.53E-05	0.000254184	2.52E-05

2) DDSCM RESULTS

The parameters extracted from the seven algorithms for DDSCM explain in table 3. Based on this data the best value of PE5DSSE is 2.51E-05, that is achieved by the TFWO algorithm, the TLBO algorithm achieve the second best PE5DSSE (2.52E-05) then MFO, CSA, GWO, TSA and MPSO respectively. Figure 9 explains the I-V and P-V curves for DDSCM at the best value of PE5DSSE from the proposed TFWO. Figure 10 explains the absolute error for current and power curves for DDSCM at the best value of PE5DSSE from the proposed TFWO. Based on these figures; the maximum absolute error for current is 0.00255209505168791, the maximum absolute error for power is 0.00148863704364956.

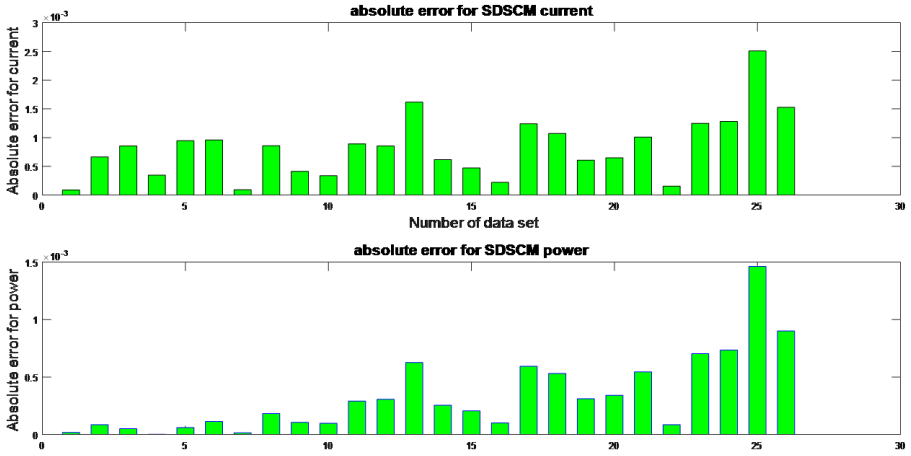

FIGURE 8. Absolute error of current and power for SDSCM at the best PE5DSSE from TFWO.

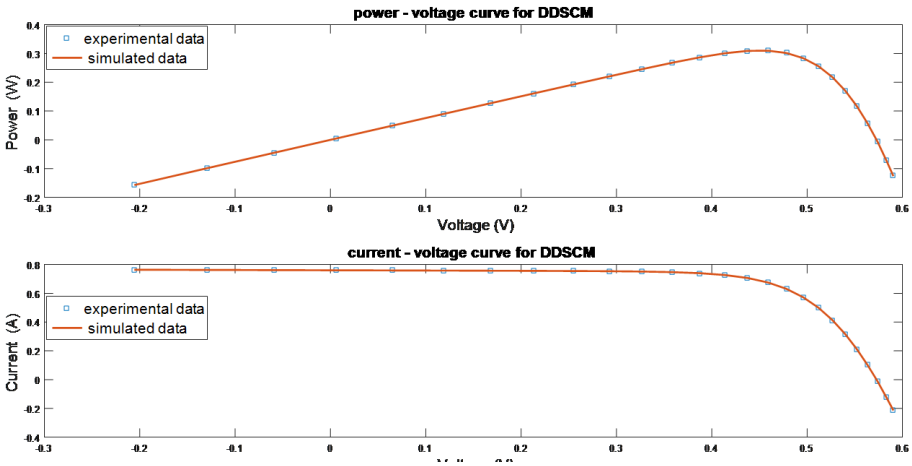

FIGURE 9. I-V and P-V curves for DDSCM at the best PE5DSSE from TFWO.

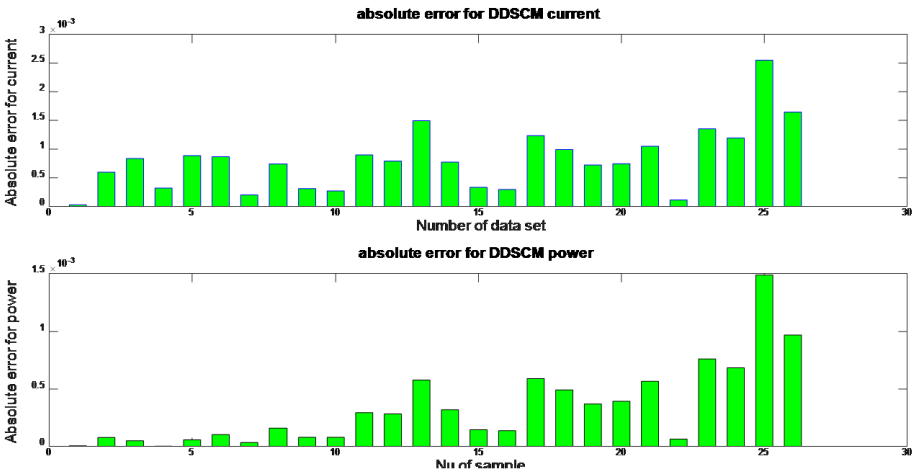

FIGURE 10. Absolute error of current and power for DDSCM at the best PE5DSSE from TFWO.

3) TDSCM RESULTS

The parameters extracted from the seven algorithms for TDSCM explain in table 4. Based on this data the best value of PE5DSSE is 2.51E-05, that is achieved by the TFWO algorithm, the TLBO algorithm achieve the second best PE5DSSE then MFO, CSA, GWO, TLBO and MPSO respectively. Figure 11 explains the I-V and P-V curves for TDSCM at the best value of PE5DSSE from the proposed TFWO.

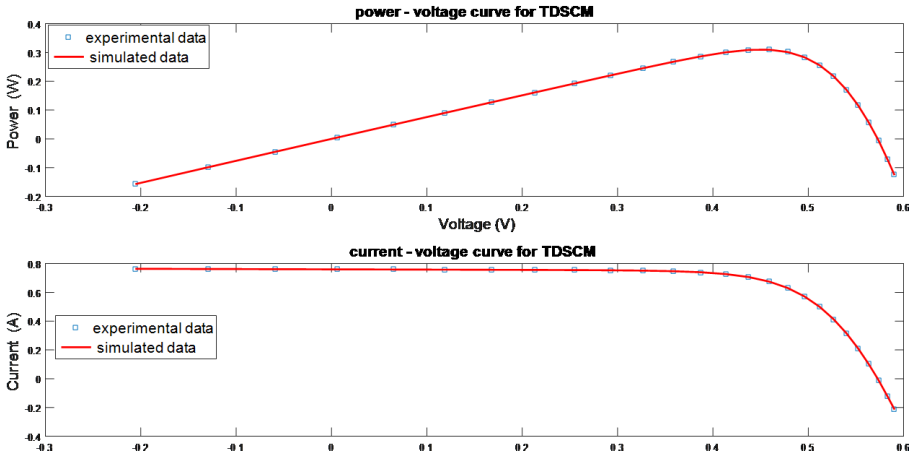

FIGURE 11. I-V and P-V curves for TDSCM at the best PE5DSSE from TFWO.

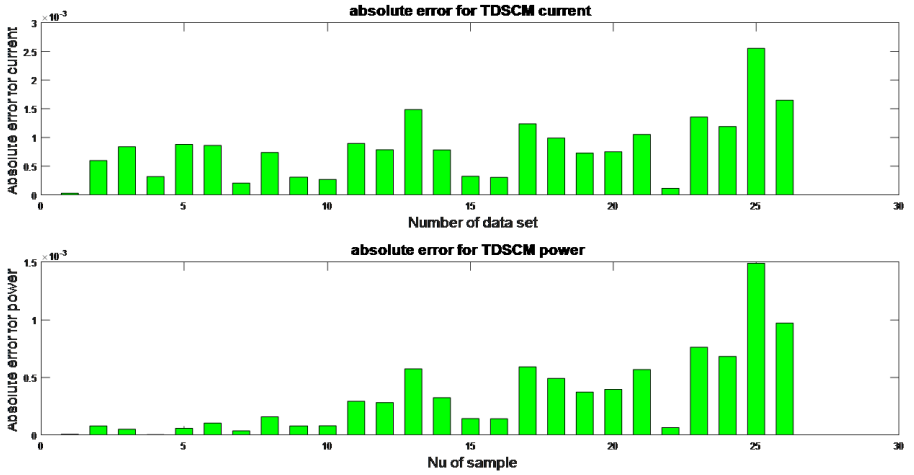

FIGURE 12. Absolute error of current and power for TDSCM at the best PE5DSSE from TFWO.

TABLE 4. The parameters identified TDSCM at the best PE5DSSE.

Algorithm	TFWO	TSA	GWO	CSA	MFO	MPSO	TLBO
I_{ph} (A)	0.760785893	7.60E-01	7.60E-01	0.76093344	7.61E-01	0.762031766	0.760762807
I_{o1} (A)	4.99E-07	2.68E-07	2.82E-07	4.05E-07	4.41E-07	1.00E-06	1.20E-08
n_1	2	1.72E+00	1.48E+00	1.97464613	1.87E+00	2	1.999999703
R_s (Ω)	0.036817601	0.035085872	0.035985297	0.03750399	0.036495991	0.028602862	0.036571816
R_{sh} (Ω)	55.77485079	84.24285936	74.46265839	49.0414703	56.23076795	100	56.28600446
I_{s2} (A)	3.89E-07	7.99E-08	2.54E-09	1.35E-07	2.28E-08	1.00E-06	6.97E-07
n_2	2	1.400034217	1.572739961	1.40803755	2	2	1.999975103
I_{s3} (A)	2.10E-07	7.96E-07	1.33E-07	4.76E-07	2.36E-07	1.00E-06	2.39E-07
n_3	1.444905007	1.721506599	1.60664476	1.863603121	1.456482764	1.622366704	1.456323391
PE5DSSE	2.51E-05	8.29E-05	3.78E-05	3.12E-05	2.53E-05	0.000379728	2.52E-05

TABLE 5. The parameters identified MSDSCM at the best PE5DSSE.

Algorithm	I_{pv} (A)	I_{o1} (A)	n_1	R_s (Ω)	R_{sh} (Ω)	R_{sm} (Ω)	PE5DSSE
TFWO	0.760774525	3.23E-07	1.48118376	0.036377085	53.7186078	0.5	2.5278E-05
TSA	0.758507147	2.63E-07	1.460665495	0.037372671	59.03332454	0.184002883	8.50E-05
GWO	0.760283705	2.84E-07	1.4679542	0.03713415	62.14773501	0.155768694	3.70E-05
CSA	0.760809548	3.35E-07	1.484786044	0.036225635	55.06343043	0.39230771	2.56E-05
MFO	0.760753734	3.38E-07	1.485881701	0.036192098	55.01960307	0.5	2.55E-05
MPSO	0.760841051	1.00E-06	1.604527024	0.031385159	100	0.5	0.000155835
TLBO	0.760776458	3.27E-07	1.482428058	0.036333485	54.16322019	0	2.5298E-05

Figure 12 explains the absolute error for current and power curves for TDSCM at the best value of PE5DSSE from the proposed TFWO. Based on these figures; the maximum absolute error for current is 0.00255165596868381, the maximum absolute error for power is 0.00148838092653328.

B. RESULTS OF THE MODIFIED SOLAR CELL MODELS

The results of the modified solar cell models, namely, MSDSCM, MDDSCM, and MTDSCM, are discussed in this subsection. The estimated parameters of these models are based on the new objective function; further, PE5DSSE for the proposed TFWO algorithm and other compared algorithms is discussed. The I–V and P–V curves for the R.T.C France solar cell are illustrated for SDSCM, DDSCM, and TDSCM using the best PE5DSSE value by employing the proposed TFWO algorithm.

1) MSDSCM RESULTS

The parameters extracted from the seven algorithms for MSDSCM are presented in Table 5. Based on these data, the best PE5DSSE value is 2.5278E-05, which is achieved using the proposed TFWO algorithm. The TLBO algorithm achieves the second-best PE5DSSE value (2.5298E-05),

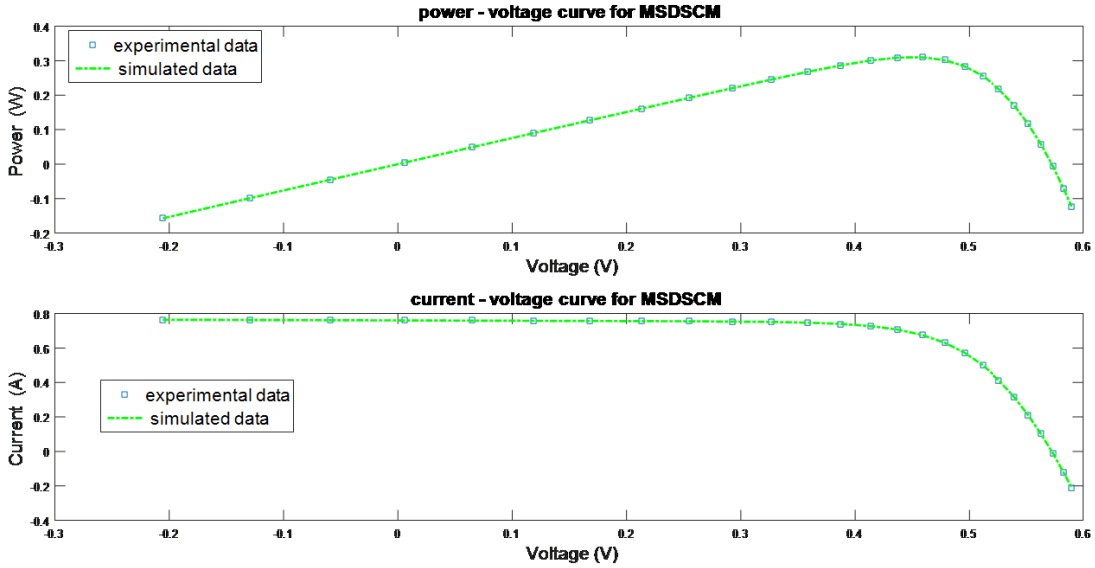

FIGURE 13. I-V and P-V curves for MSDSCM at the best PE5DSSE from TFWO.

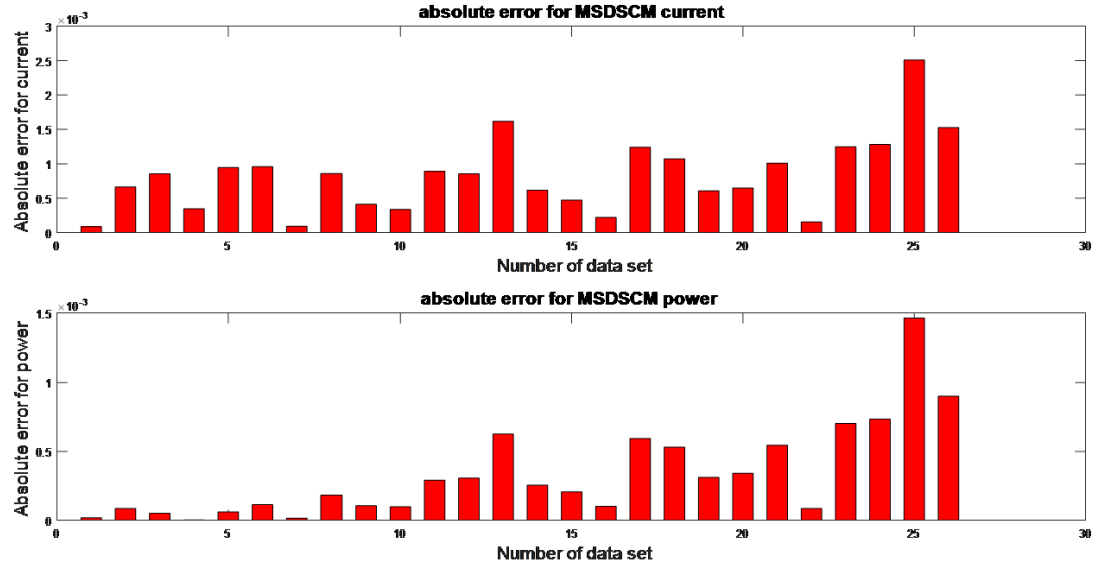

FIGURE 14. Absolute error of current and power for MSDSCM at the best PE5DSSE from TFWO.

followed by CSA, MFO, GWO, TSA, and MPSO, in the given order. Figure 13 presents the I–V and P–V curves for SDSCM using the best PE5DSSE value by employing the proposed TFWO algorithm. Figure 14 shows the absolute error of the current and power curves for SDSCM using the best PE5DSSE value by employing the proposed TFWO algorithm. Based on these figures, the maximum absolute errors of the current and power curves are 0.00250741122972475 and 0.00146257297029845, respectively.

2) MDDSCM RESULTS

The parameters extracted from the seven algorithms for DDSCM explain in table 6. Based on this data the best value of PE5DSSE is 2.51E-05, that is achieved by the TFWO algorithm, the TLBO algorithm achieve the second best PE5DSSE (2.522E-05) then MFO, CSA, GWO, TSA and MPSO respectively. Figure 15 explains the I-V and P-V curves for DDSCM at the best value of PE5DSSE from the proposed TFWO. Figure 16 presents the absolute error of the current and power curves for DDSCM using the best PE5DSSE value by employing the proposed TFWO algorithm. Based on these figures, the maximum absolute errors of the current and power curves are 0.00254956327080924 and 0.00148716025586303, respectively.

3) MTDSCM RESULTS

The parameters extracted from the seven algorithms for MTDSCM explain in table7. Based on these data, the best

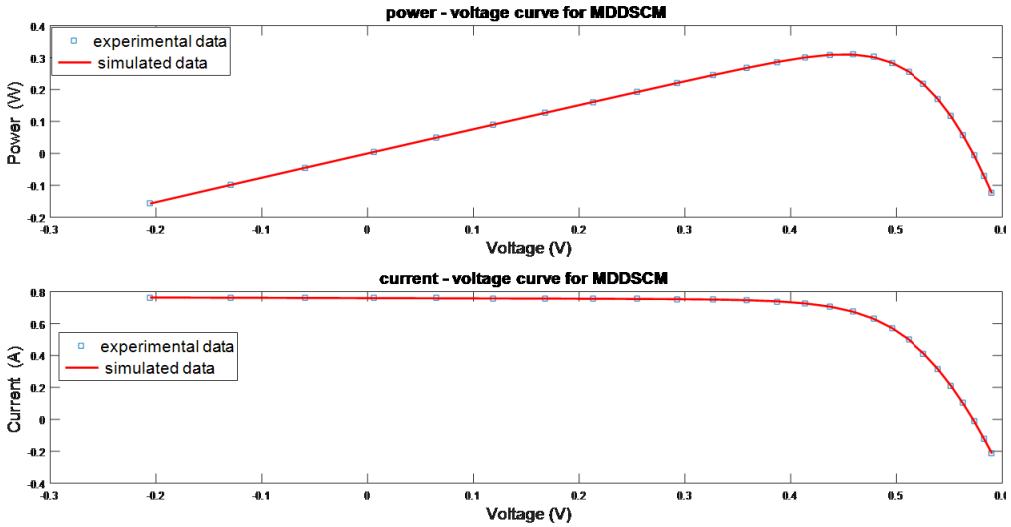

FIGURE 15. I-V and P-V curves for MDDSCM at the best PE5DSSE from TFWO.

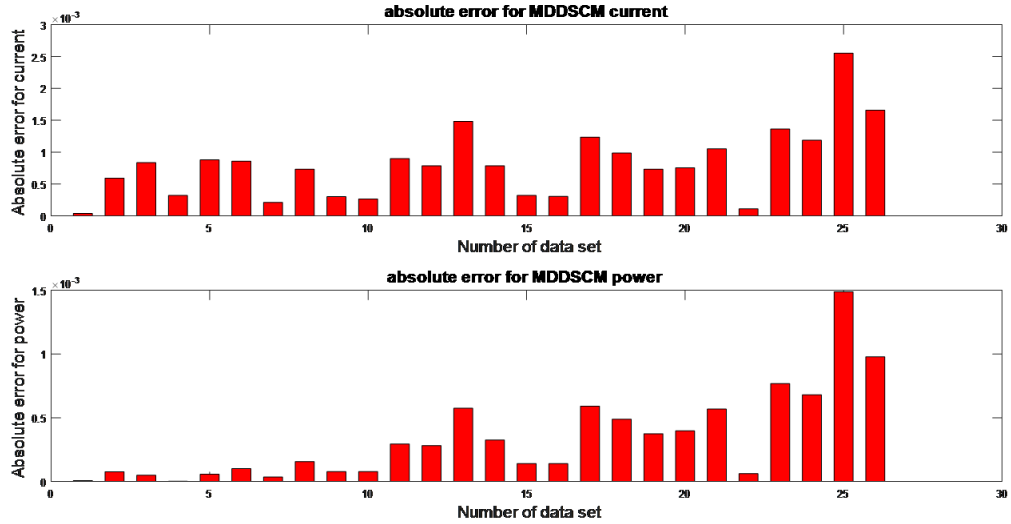

FIGURE 16. Absolute error of current and power for MDDSCM at the best PE5DSSE from TFWO.

TABLE 6. The parameters identified MDDSCM at the best PE5DSSE.

Algorithm	TFWO	TSA	GWO	CSA	MFO	MPSO	TLBO
I_{ph} (A)	0.760783023	0.760536993	0.760368397	0.760815765	0.76077288	0.76145492	0.760772562
I_{o1} (A)	9.17E-07	1.92E-07	6.41E-08	1.00E-06	9.91E-07	1.00E-06	1.27E-07
n_1	1.999992291	1.43047132	1.488340483	2	1.793121527	2	1.999999997
R_s (Ω)	0.036835645	0.039448891	0.035758652	0.037353623	0.037266945	0.030003295	0.036419281
R_{sh} (Ω)	55.8909553	58.32796952	60.50580591	56.74720283	58.36815389	100	54.11391541
I_{s2} (A)	2.07E-07	7.85E-10	3.23E-07	1.77E-07	8.11E-08	1.00E-06	3.06E-07
n_2	1.443600817	1.516566902	1.501956165	1.429401022	1.376906108	1.613065756	1.476708608
R_{sm} (Ω)	0.01025276	0.064407069	0.215263208	0.117328777	0.5	0.5	0.5
PE5DSSE	2.51E-05	0.000130439	3.07E-05	3.03E-05	2.59E-05	0.00025418	2.52E-05

TABLE 7. The parameters identified MTDSCM at the best PE5DSSE.

Algorithm	TFWO	TSA	GWO	CSA	MFO	MPSO	TLBO
I_{ph} (A)	0.760780283	7.60E-01	0.760101592	0.761275488	0.760708173	0.76203075	0.760758541
I_{o1} (A)	7.63E-07	8.66E-08	4.37E-07	5.66E-07	0.00E+00	1.00E-06	3.28E-08
n_1	2	1.39E+00	1.636352326	1.999796688	2	2	1.964032638
R_s (Ω)	0.036749141	0.037929107	0.036125616	0.036700238	0.035983445	0.028602919	0.03680679
R_{sh} (Ω)	55.52672891	94.90232731	75.28225626	55.49900285	58.18521753	100	56.22071282
I_{o2} (A)	2.47E-09	4.78E-07	2.26E-08	1.84E-07	2.30E-07	1.00E-06	2.09E-07
n_2	2	1.853504255	1.945023864	1.434568733	1.900984751	2	1.444515189
I_{o3} (A)	2.24E-07	2.99E-07	1.14E-07	6.55E-07	3.17E-07	1.00E-06	8.64E-07
n_3	1.450312839	1.639978259	1.419854441	2	1.481921974	1.622365286	1.998818184
R_{sm} (Ω)	0.5	0.318780538	0.212811561	4.09E-01	0.5	0.5	0.378126666
PE5DSSE	2.509E-05	0.000112853	3.88E-05	3.03E-05	2.68E-05	0.000379723	2.51E-05

PE5DSSE value is 2.509E-05, which is achieved using the TFWO algorithm. The TLBO algorithm achieves the second-best PE5DSSE value, followed by MFO, CSA, GWO, TLBO, and MPSO, in the given order. Figure 17 shows the I–V and P–V curves for TDSCM using the best PE5DSSE value by employing the proposed TFWO algorithm. Figure 18 shows the absolute error of the current and power curves for TDSCM using the best PE5DSSE value by employing the proposed TFWO algorithm. Based on these figures, the maximum absolute errors of the current and power curves are 0.00254473384254822 and 0.00148434325035837, respectively.

C. STATISTICAL ANALYSIS FOR ROBUSTNESS DATA FOR ALL ALGORITHMS

In this section, we compared the performance of the modified and traditional solar cell models. The accuracy and

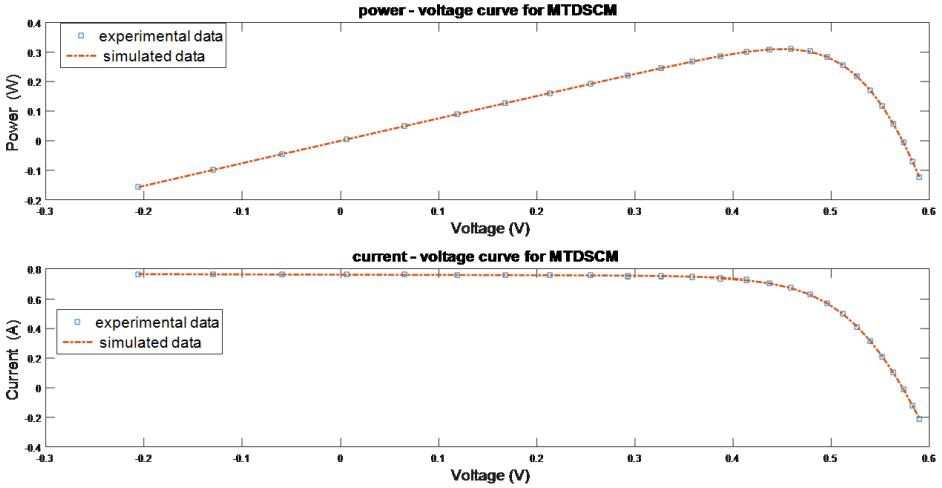

FIGURE 17. I-V and P-V curves for MTDSCM at the best PE5DSSE from TFWO.

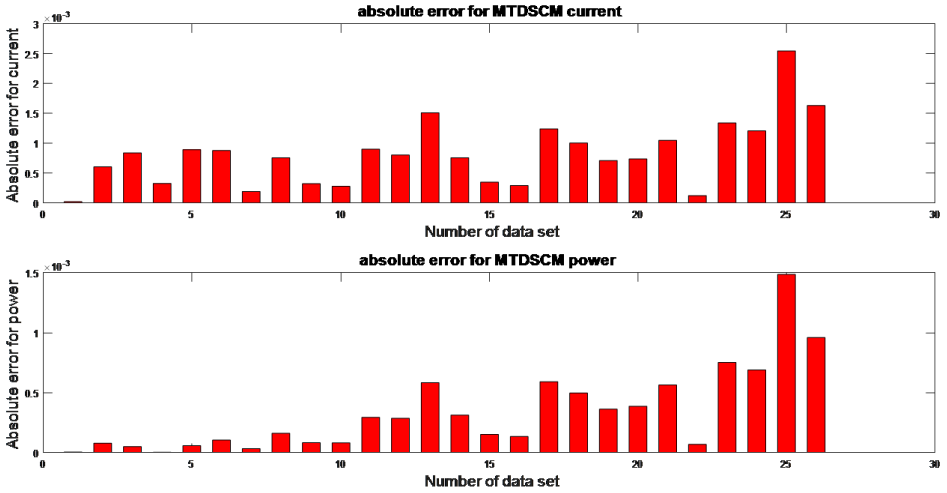

FIGURE 18. Absolute error of current and power for MTDSCM at the best PE5DSSE from TFWO.

TABLE 8. Statistical data for SDSCM and MSDSCM.

SDSCM							
Algorithm	**TFWO**	**TSA**	**GWO**	**CSA**	**MFO**	**MPSO**	**TLBO**
Minimum	2.52788E-05	1.03E-04	4.66E-05	2.55E-05	2.56E-05	0.000155841	2.5308E-05
Mean	2.5279E-05	0.003834799	0.002499712	2.88E-05	9.15E-05	0.004704237	3.94E-05
Maximum	2.52794E-05	0.056305125	0.03867791	4.29E-05	0.000155841	0.058255295	0.000105334
SD	1.38E-10	0.012216158	0.008198963	3.60E-06	5.27E-05	0.014171927	1.89E-05
MSDSCM							
Algorithm	**TFWO**	**TSA**	**GWO**	**CSA**	**MFO**	**MPSO**	**TLBO**
Minimum	2.5278E-05	8.50E-05	3.70E-05	2.56E-05	2.55E-05	000155835	2.52E-05
Mean	2.5279E-05	0.002090221	0.009165125	2.86E-05	0.003370458	0.006685213	3.16E-05
Maximum	2.52792E-05	0.042215462	0.0569412	3.67E-05	0.058255295	0.039332228	6.25E-05
SD	2.56E-11	0.007613273	0.017746795	2.67E-06	0.012595125	0.014849722	1.05E-05

TABLE 9. Statistical data for DDSCM and MDDSCM.

DDSCM							
Algorithm	**TFWO**	**TSA**	**GWO**	**CSA**	**MFO**	**MPSO**	**TLBO**
Minimum	2.51E-05	0.000133951	6.27E-05	2.88E-05	2.53E-05	0.000254184	2.52E-05
Mean	2.53E-05	0.003393458	0.008126224	5.40E-05	0.003305654	0.003775853	4.13E-05
Maximum	2.63E-05	0.039928833	0.044249601	0.000115394	0.035470873	0.035470873	8.13E-05
SD	2.49E-07	0.009850679	0.015335808	2.11E-05	0.009681063	0.010745618	1.65E-05
MDDSCM							
Algorithm	**TFWO**	**TSA**	**GWO**	**CSA**	**MFO**	**MPSO**	**TLBO**
Minimum	2.51E-05	0.000130439	3.07E-05	3.03E-05	2.59E-05	0.00025418	2.52E-05
Mean	2.53E-05	0.003231123	0.003245681	5.29E-05	0.002114365	0.00973519	3.53E-05
Maximum	2.61E-05	0.044413563	0.041608648	0.000210514	0.029856949	0.042254923	7.39E-05
SD	1.53E-07	0.009908143	1.11E-02	4.66E-05	0.007541592	0.014903679	1.27E-05

TABLE 10. Statistical data for TDSCM and MTDSCM.

TDSCM							
Algorithm	**TFWO**	**TSA**	**GWO**	**CSA**	**MFO**	**MPSO**	**TLBO**
Minimum	2.51E-05	8.29E-05	3.78E-05	3.12E-05	2.53E-05	0.000379728	2.52E-05
Mean	2.54E-05	0.003342881	0.009509075	7.49E-05	0.002066078	0.004887584	4.41E-05
Maximum	2.72E-05	0.042177587	0.056090156	0.000153084	0.0319076	0.037784521	0.000115186
SD	4.21E-07	0.009675626	0.015720233	3.52E-05	0.007212398	0.010475286	1.73E-05
MTDSCM							
Algorithm	**TFWO**	**TSA**	**GWO**	**CSA**	**MFO**	**MPSO**	**TLBO**
Minimum	2.509E-05	1.13E-04	3.88E-05	3.03E-05	2.68E-05	0.000379723	2.51E-05
Mean	2.53E-05	0.002375018	0.003961363	9.28E-05	0.001042276	0.008258652	3.46E-05
Maximum	2.56E-05	0.034251289	0.038357238	0.000210514	0.024842906	0.031907633	0.000116713
SD	8.20E-08	0.006207975	1.11E-02	4.66E-05	0.004496967	0.012299616	1.74E-05

reliability of each model are compared. The accuracy of the model is measured using the best PE5DSSE value. The reliability of the model is measured using the standard deviations of 30 independent runs for each model based on the PE5DSSE value. The minimum, mean, maximum, and standard deviation values of all the algorithms for SDSCM and MSDSCM are presented in Table 8, those for DDSCM and MDDSCM are shown in Table 9, and those for SDSCM and MSDSCM are presented in Table 10. The results provided in Tables 7, 8, and 9 show that MSDSCM is more accurate and reliable than SDSCM. Furthermore, MDDSCM and MTDSCM are more reliable and accurate than DDSCM and TDSCM, respectively. The proposed TFWO algorithm

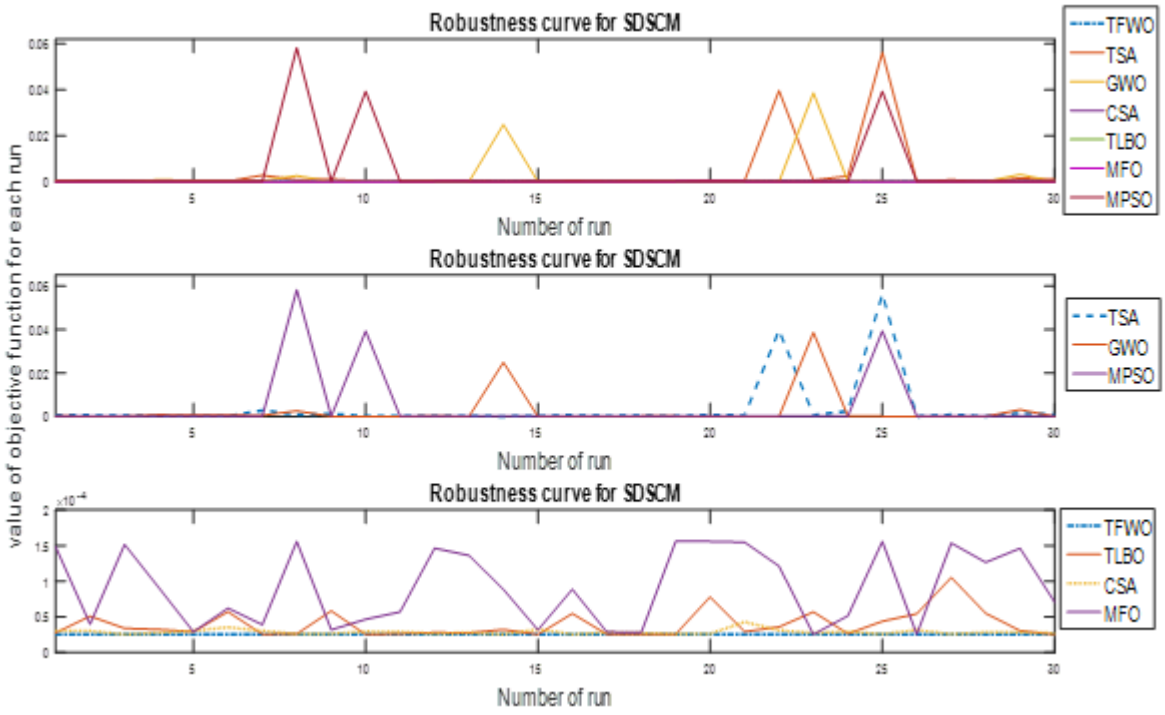

FIGURE 19. The SDSCM robustness data.

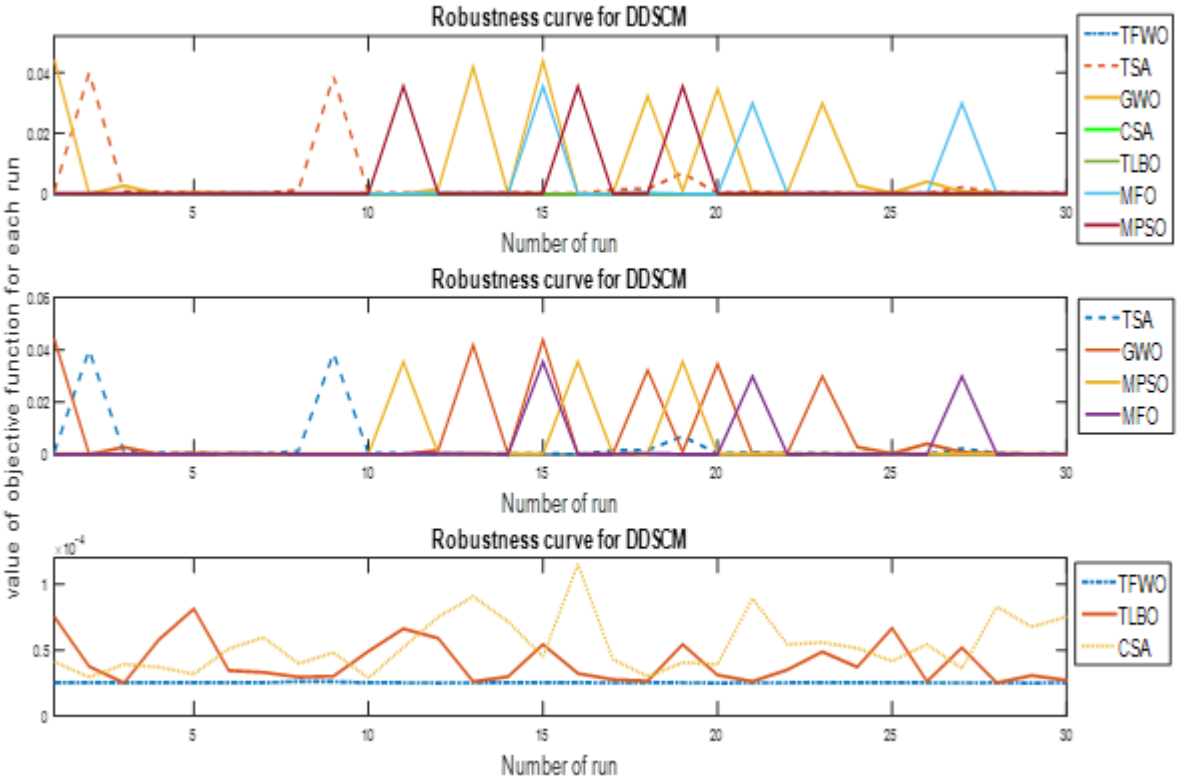

FIGURE 20. The DDSCM robustness data.

achieves the optimal results for the minimum, mean, maximum, and standard deviation values using PE5DSSE compared with other algorithms.

We performed statistical analysis for 30 independent runs for all algorithms. The robustness curves for TFWO, TSA, GWO, CSA, MFO, MPSO, and TLBO are presented in

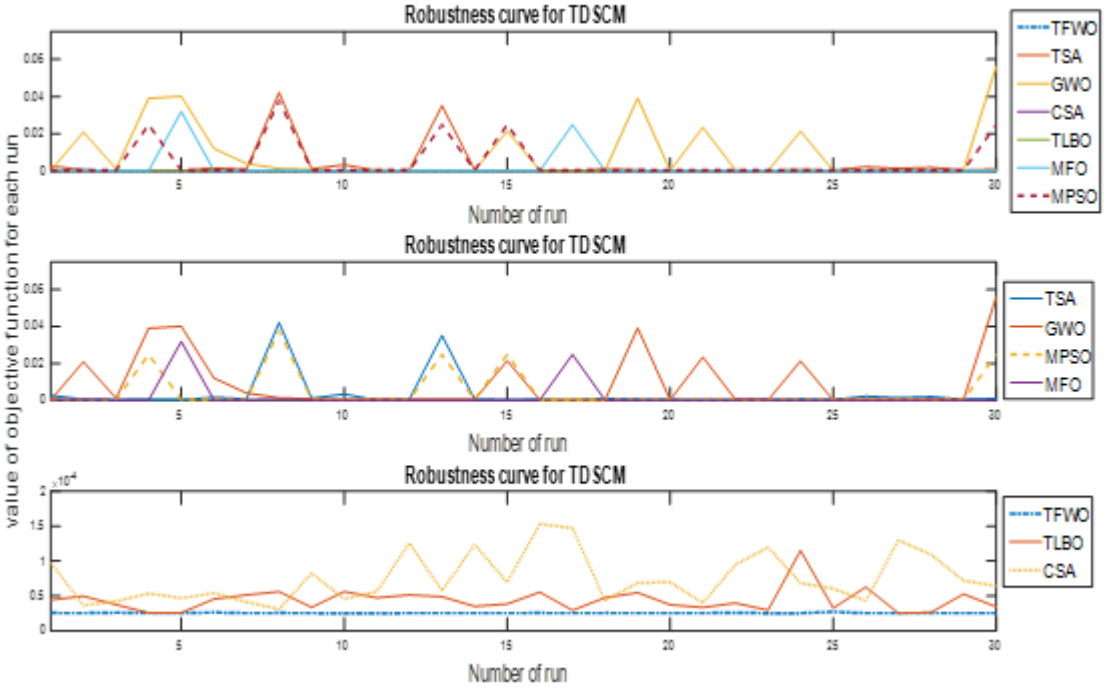

FIGURE 21. The TDSCM robustness data.

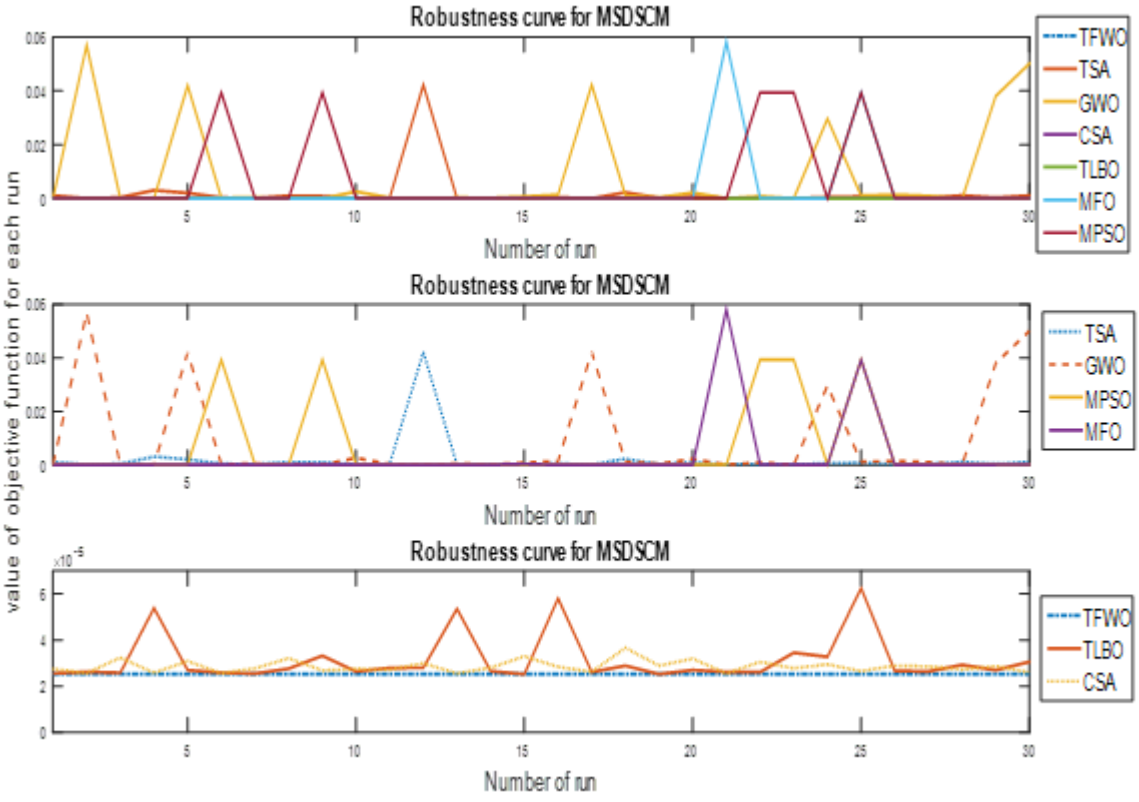

FIGURE 22. The MSDSCM robustness data.

Figures 19, 20, 21, 22, 23 and 24 for SDSCM, DDSCM, TDSCM, MSDSCM, MDDSCM, and MTDSCM, respectivelyi. Based on these figures, the objective function output from each run for most algorithms diverges from the best solution, except for the solutions extracted using the proposed TFWO algorithm. The global optimum solution is converged by the proposed TFWO. Therefore, the TFWO algorithm is superior to all comparative algorithms.

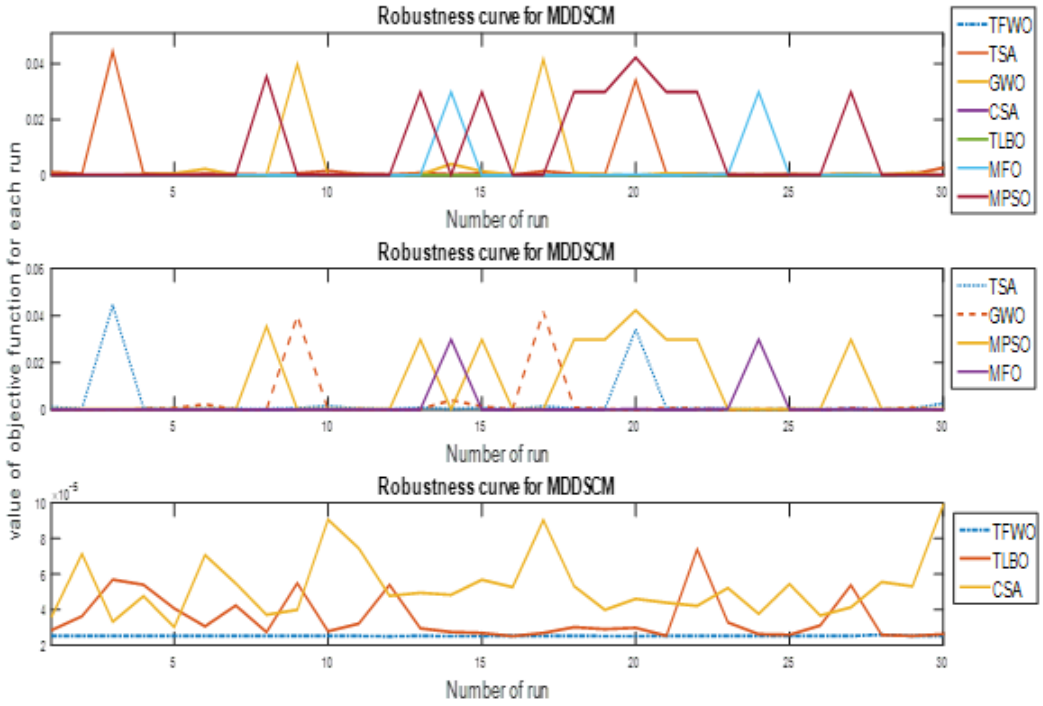

FIGURE 23. The MDDSCM robustness data.

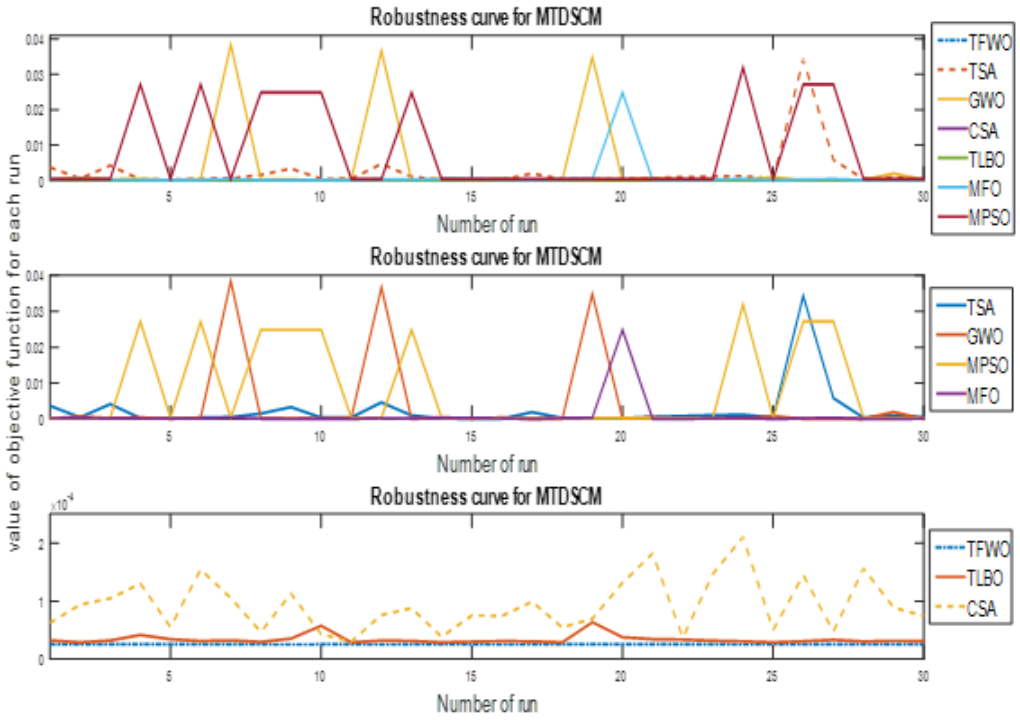

FIGURE 24. The MTDSCM robustness data.

VI. CONCLUSION AND FUTURE WORK

The PV systems are becoming one of the most popular renewable energy technologies for generating electric power. Establishing an accurate PV model that emulates the system behavior under different environmental conditions is essential. The challenge of PV cell parameter estimation has garnered the attention of researchers and industrialists and gained immense momentum for the development of PV models. The accuracy of the PV model depends on its identified parameters that are mainly based on the executed optimization technique and employed objective function. Therefore, we use PE5DSSE between the measured and calculated

currents. PE5DSSE is used as a new objective function for extracting the parameters of the solar cell models. Herein, we present an efficient MH method, called TFWO, for estimating the parameters of PVs in solar cell systems. Regarding the proposed objective function, the experimental and comparative results show that TFWO with high stability achieves more precise and accurate parameters than other competitor algorithms. The main conclusions of this study are listed:

- We propose a new objective function based on polynomial equations to extract the parameters of the solar cell models.
- This function yields the most accurate, precise, and consistent solutions.
- The modified solar cell models, namely, MSDSCM, MDDSCM, and MTDSCM, are more accurate and reliable than the traditional solar cell models, namely, SDSCM, DDSCM, and TDSCM.
- TFWO shows more flexibility and effectiveness performance than the other algorithms.
- The good fit confirms the superior reliability and stability of TFWO.
- The superiority of the TFWO algorithm in comparison with other competitor algorithms is confirmed in terms of the experimental dataset fitting accuracy, convergence rate, stability, and consistency of the results.

the future, we aim to improve the TFWO and other MH algorithms for enhanced renewable energy and power systems. Moreover, we will consider the output power prediction of multiple energy systems under the integrated energy system. We also aim to perform research on the optimal control of energy internet.

CONFLICT OF INTEREST

The authors declare that there is no conflict of interest.

CREDiT AUTHOR STATEMENT

All authors contributed equally to this paper, where; Diaa Salama AbdElminaam: Software, Methodology, Conceptualization, Formal analysis, Writing - review & editing. Mokhtar Said: Software, Resources, Writing - original draft, Methodology, Data curation, Formal analysis. Essam H. Houssein: Supervision, Software, Methodology, Conceptualization, Formal analysis, Writing - review & editing. All authors read and approved the final paper.

REFERENCES

[1] M. Abdel-Basset, D. El-Shahat, R. K. Chakrabortty, and M. Ryan, "Parameter estimation of photovoltaic models using an improved marine predators algorithm," *Energy Convers. Manage.*, vol. 227, Jan. 2021, Art. no. 113491.

[2] A. Nadeem, H. A. Sher, A. F. Murtaza, and N. Ahmed, "Online current-sensorless estimator for PV open circuit voltage and short circuit current," *Sol. Energy*, vol. 213, pp. 198–210, Jan. 2021.

[3] M. H. Qais, H. M. Hasanien, S. Alghuwainem, and A. S. Nouh, "Coyote optimization algorithm for parameters extraction of three-diode photovoltaic models of photovoltaic modules," *Energy*, vol. 187, Nov. 2019, Art. no. 116001.

[4] F. A. Hashim, K. Hussain, E. H. Houssein, M. S. Mabrouk, and W. Al-Atabany, "Archimedes optimization algorithm: A new metaheuristic algorithm for solving optimization problems," *Appl. Intell.*, vol. 51, pp. 1531–1551, Sep. 2020.

[5] M. M. Ahmed, E. H. Houssein, A. E. Hassanien, A. Taha, and E. Hassanien, "Maximizing lifetime of large-scale wireless sensor networks using multi-objective whale optimization algorithm," *Telecommun. Syst.*, vol. 72, no. 2, pp. 243–259, Oct. 2019.

[6] A. A. K. Ismaeel, E. H. Houssein, D. Oliva, and M. Said, "Gradient-based optimizer for parameter extraction in photovoltaic models," *IEEE Access*, vol. 9, pp. 13403–13416, 2021.

[7] K. Ishaque, Z. Salam, S. Mekhilef, and A. Shamsudin, "Parameter extraction of solar photovoltaic modules using penalty-based differential evolution," *Appl. Energy*, vol. 99, pp. 297–308, Nov. 2012.

[8] M. A. Soliman, H. M. Hasanien, and A. Alkuhayli, "Marine predators algorithm for parameters identification of triple-diode photovoltaic models," *IEEE Access*, vol. 8, pp. 155832–155842, 2020.

[9] Y. Zhang, Z. Jin, and S. Mirjalili, "Generalized normal distribution optimization and its applications in parameter extraction of photovoltaic models," *Energy Convers. Manage.*, vol. 224, Nov. 2020, Art. no. 113301.

[10] S. Kaur, L. K. Awasthi, A. L. Sangal, and G. Dhiman, "Tunicate swarm algorithm: A new bio-inspired based Metaheuristic paradigm for global optimization," *Eng. Appl. Artif. Intell.*, vol. 90, Apr. 2020, Art. no. 103541.

[11] D. Yousri, D. Allam, T. S. Babu, A. M. Abdelaty, A. G. Radwan, V. K. Ramachandaramurthy, and M. B. Eteiba, "Fractional chaos maps with flower pollination algorithm for chaotic systems' parameters identification," *Neural Comput. Appl.*, vol. 32, no. 20, pp. 16291–16327, Oct. 2020.

[12] A. Abbassi, R. Abbassi, A. A. Heidari, D. Oliva, H. Chen, A. Habib, M. Jemli, and M. Wang, "Parameters identification of photovoltaic cell models using enhanced exploratory salp chains-based approach," *Energy*, vol. 198, May 2020, Art. no. 117333.

[13] Y. Wu, R. Chen, C. Li, L. Zhang, and Z. Cui, "Hybrid symbiotic differential evolution moth-flame optimization algorithm for estimating parameters of photovoltaic models," *IEEE Access*, vol. 8, pp. 156328–156346, 2020.

[14] E. I. Batzelis and S. A. Papathanassiou, "A method for the analytical extraction of the single-diode PV model parameters," *IEEE Trans. Sustain. Energy*, vol. 7, no. 2, pp. 504–512, Apr. 2016.

[15] M. Hejri, H. Mokhtari, M. R. Azizian, M. Ghandhari, and L. Söder, "On the parameter extraction of a five-parameter double-diode model of photovoltaic cells and modules," *IEEE J. Photovolt.*, vol. 4, no. 3, pp. 915–923, May 2014.

[16] G. Xian-Kun, Y. Chuan-An, G. Xiang-Chuan, and Y. Yong-Chang, "Accuracy comparison between implicit and explicit single-diode models of photovoltaic cells and modules," *Acta Phys. Sinica*, vol. 63, no. 17, 2014, Art. no. 178401.

[17] F. Dkhichi, B. Oukarfi, A. Fakkar, and N. Belbounaguia, "Parameter identification of solar cell model using Levenberg–Marquardt algorithm combined with simulated annealing," *Sol. Energy*, vol. 110, pp. 781–788, Dec. 2014.

[18] M. Chegaar, Z. Ouennoughi, and A. Hoffmann, "A new method for evaluating illuminated solar cell parameters," *Solid-State Electron.*, vol. 45, no. 2, pp. 293–296, Feb. 2001.

[19] D. F. Alam, D. A. Yousri, and M. B. Eteiba, "Flower pollination algorithm based solar PV parameter estimation," *Energy Convers. Manage.*, vol. 101, pp. 410–422, Sep. 2015.

[20] F. A. Hashim, E. H. Houssein, K. Hussain, M. S. Mabrouk, and W. Al-Atabany, "A modified Henry gas solubility optimization for solving motif discovery problem," *Neural Comput. Appl.*, vol. 32, no. 14, pp. 10759–10771, Jul. 2020.

[21] E. H. Houssein, M. E. Hosney, D. Oliva, W. M. Mohamed, and M. Hassaballah, "A novel hybrid harris hawks optimization and support vector machines for drug design and discovery," *Comput. Chem. Eng.*, vol. 133, Feb. 2020, Art. no. 106656.

[22] N. Neggaz, E. H. Houssein, and K. Hussain, "An efficient Henry gas solubility optimization for feature selection," *Expert Syst. Appl.*, vol. 152, Aug. 2020, Art. no. 113364.

[23] P. A. Kumari and P. Geethanjali, "Adaptive genetic algorithm based multi-objective optimization for photovoltaic cell design parameter extraction," *Energy Procedia*, vol. 117, pp. 432–441, Jun. 2017.

[24] D. H. Muhsen, A. B. Ghazali, T. Khatib, and I. A. Abed, "Extraction of photovoltaic module model's parameters using an improved hybrid differential evolution/electromagnetism-like algorithm," *Sol. Energy*, vol. 119, pp. 286–297, Sep. 2015.

[25] B. Yang, T. Yu, X. Zhang, H. Li, H. Shu, Y. Sang, and L. Jiang, "Dynamic leader based collective intelligence for maximum power point tracking of PV systems affected by partial shading condition," *Energy Convers. Manage.*, vol. 179, pp. 286–303, Jan. 2019.

[26] X. Chen, B. Xu, C. Mei, Y. Ding, and K. Li, "Teaching–learning–based artificial bee colony for solar photovoltaic parameter estimation," *Appl. Energy*, vol. 212, pp. 1578–1588, Feb. 2018.
[27] M. Amroune, T. Bouktir, and I. Musirin, "Power system voltage instability risk mitigation via emergency demand response-based whale optimization algorithm," *Protection Control Mod. Power Syst.*, vol. 4, no. 1, p. 25, Dec. 2019.
[28] O. S. Elazab, H. M. Hasanien, M. A. Elgendy, and A. M. Abdeen, "Parameters estimation of single- and multiple-diode photovoltaic model using whale optimisation algorithm," *IET Renew. Power Gener.*, vol. 12, no. 15, pp. 1755–1761, Nov. 2018.
[29] D. Oliva, M. A. El Aziz, and A. E. Hassanien, "Parameter estimation of photovoltaic cells using an improved chaotic whale optimization algorithm," *Appl. Energy*, vol. 200, pp. 141–154, Aug. 2017.
[30] Z. Wu, D. Yu, and X. Kang, "Parameter identification of photovoltaic cell model based on improved ant lion optimizer," *Energy Convers. Manage.*, vol. 151, pp. 107–115, Nov. 2017.
[31] I. Boussaïd, A. Chatterjee, P. Siarry, and M. Ahmed-Nacer, "Biogeography-based optimization for constrained optimization problems," *Comput. Oper. Res.*, vol. 39, no. 12, pp. 3293–3304, Dec. 2012.
[32] J. Ma, T. O. Ting, K. L. Man, N. Zhang, S.-U. Guan, and P. W. H. Wong, "Parameter estimation of photovoltaic models via cuckoo search," *J. Appl. Math.*, vol. 2013, pp. 1–8, Aug. 2013.
[33] X. Chen and K. Yu, "Hybridizing cuckoo search algorithm with biogeography-based optimization for estimating photovoltaic model parameters," *Sol. Energy*, vol. 180, pp. 192–206, Mar. 2019.
[34] A. Askarzadeh and A. Rezazadeh, "Extraction of maximum power point in solar cells using bird mating optimizer-based parameters identification approach," *Sol. Energy*, vol. 90, pp. 123–133, Apr. 2013.
[35] A. Askarzadeh and L. dos Santos Coelho, "Determination of photovoltaic modules parameters at different operating conditions using a novel bird mating optimizer approach," *Energy Convers. Manage.*, vol. 89, pp. 608–614, Jan. 2015.
[36] J. P. Ram, T. S. Babu, T. Dragicevic, and N. Rajasekar, "A new hybrid bee pollinator flower pollination algorithm for solar PV parameter estimation," *Energy Convers. Manage.*, vol. 135, pp. 463–476, Mar. 2017.
[37] B. Nayak, A. Mohapatra, and K. B. Mohanty, "Parameter estimation of single diode PV module based on GWO algorithm," *Renew. Energy Focus*, vol. 30, pp. 1–12, Sep. 2019.
[38] M. A. Awadallah, "Variations of the bacterial foraging algorithm for the extraction of PV module parameters from nameplate data," *Energy Convers. Manage.*, vol. 113, pp. 312–320, Apr. 2016.
[39] B. Jacob, K. Balasubramanian, S. Babu T, S. M. Azharuddin, and N. Rajasekar, "Solar PV modelling and parameter extraction using artificial immune system," *Energy Procedia*, vol. 75, pp. 331–336, Aug. 2015.
[40] A. H. Elsheikh and M. A. Elaziz, "Review on applications of particle swarm optimization in solar energy systems," *Int. J. Environ. Sci. Technol.*, vol. 16, no. 2, pp. 1159–1170, Feb. 2019.
[41] X. Yuan, Y. Xiang, and Y. He, "Parameter extraction of solar cell models using mutative-scale parallel chaos optimization algorithm," *Sol. Energy*, vol. 108, pp. 238–251, Oct. 2014.
[42] K. M. El-Naggar, M. R. AlRashidi, M. F. AlHajri, and A. K. Al-Othman, "Simulated annealing algorithm for photovoltaic parameters identification," *Sol. Energy*, vol. 86, no. 1, pp. 266–274, Jan. 2012.
[43] T. S. Babu, J. P. Ram, K. Sangeetha, A. Laudani, and N. Rajasekar, "Parameter extraction of two diode solar PV model using fireworks algorithm," *Sol. Energy*, vol. 140, pp. 265–276, Dec. 2016.
[44] Q. Niu, H. Zhang, and K. Li, "An improved TLBO with elite strategy for parameters identification of PEM fuel cell and solar cell models," *Int. J. Hydrogen Energy*, vol. 39, no. 8, pp. 3837–3854, Mar. 2014.
[45] N. Pourmousa, S. M. Ebrahimi, M. Malekzadeh, and M. Alizadeh, "Parameter estimation of photovoltaic cells using improved lozi map based chaotic optimization algorithm," *Sol. Energy*, vol. 180, pp. 180–191, Mar. 2019.
[46] A. Askarzadeh and A. Rezazadeh, "Parameter identification for solar cell models using harmony search-based algorithms," *Sol. Energy*, vol. 86, no. 11, pp. 3241–3249, Nov. 2012.
[47] S. J. Patel, A. K. Panchal, and V. Kheraj, "Extraction of solar cell parameters from a single current–voltage characteristic using teaching learning based optimization algorithm," *Appl. Energy*, vol. 119, pp. 384–393, Apr. 2014.
[48] K. Yu, J. J. Liang, B. Y. Qu, Z. Cheng, and H. Wang, "Multiple learning backtracking search algorithm for estimating parameters of photovoltaic models," *Appl. Energy*, vol. 226, pp. 408–422, Sep. 2018.
[49] M. F. AlHajri, K. M. El-Naggar, M. R. AlRashidi, and A. K. Al-Othman, "Optimal extraction of solar cell parameters using pattern search," *Renew. Energy*, vol. 44, pp. 238–245, Aug. 2012.
[50] Y. Chen, Z. Chen, L. Wu, C. Long, P. Lin, and S. Cheng, "Parameter extraction of PV models using an enhanced shuffled complex evolution algorithm improved by opposition-based learning," *Energy Procedia*, vol. 158, pp. 991–997, Feb. 2019.
[51] S. Kaur, L. K. Awasthi, A. L. Sangal, and G. Dhiman, "Tunicate swarm algorithm: A new bio-inspired based metaheuristic paradigm for global optimization," *Eng. Appl. Artif. Intell.*, vol. 90, Apr. 2020, Art. no. 103541.
[52] S. Mirjalili, S. M. Mirjalili, and A. Lewis, "Grey wolf optimizer," *Adv. Eng. Softw.*, vol. 69, pp. 46–61, Mar. 2014.
[53] L. Yitong, F. Mengyin, and G. Hongbin, "A modified particle swarm optimization algorithm," in *Proc. Chin. Control Conf.*, Jul. 2006, pp. 479–483.
[54] A. H. Gandomi, X.-S. Yang, and A. H. Alavi, "Cuckoo search algorithm: A metaheuristic approach to solve structural optimization problems," *Eng. Comput.*, vol. 29, no. 1, pp. 17–35, Jan. 2013.
[55] S. Mirjalili, "Moth-flame optimization algorithm: A novel nature-inspired heuristic paradigm," *Knowl.-Based Syst.*, vol. 89, pp. 228–249, Nov. 2015.
[56] R. V. Rao, V. J. Savsani, and D. P. Vakharia, "Teaching–learning-based optimization: An optimization method for continuous non-linear large scale problems," *Inf. Sci.*, vol. 183, no. 1, pp. 1–15, Jan. 2012.
[57] M. Ghasemi, I. F. Davoudkhani, E. Akbari, A. Rahimnejad, S. Ghavidel, and L. Li, "A novel and effective optimization algorithm for global optimization and its engineering applications: Turbulent flow of water-based optimization (TFWO)," *Eng. Appl. Artif. Intell.*, vol. 92, Jun. 2020, Art. no. 103666.

DIAA SALAMA ABDELMINAAM received the Ph.D. degree in information system from the Faculty of Computers and Information, Menufia University, Egypt, in 2015. Since February 2020, he has been an Associate Professor with the Information Systems Department, Faculty of Computers and Information, Benha University, Egypt. He has worked on several research topics. He has contributed more than 60+ technical articles in the areas of wireless networks, wireless network security, information security and Internet applications, cloud computing, mobile cloud computing, the Internet of Things, optimization, meta-heuristic algorithms, and machine learning in international journals, international conferences, local journals, and local conferences. He majors in cryptography, network security, the IoT, big data, cloud computing, and deep learning.

MOKHTAR SAID received the B.Sc. degree (Hons.) in electrical engineering, and the M.Sc. and Ph.D. degrees from the Faculty of Engineering, Fayoum University, Egypt, in June 2009, September 2013, and 2018, respectively. His major research interests include modeling and simulation of electrical systems, and electrical drives control and optimization of renewable energy systems.

ESSAM H. HOUSSEIN received the Ph.D. degree in computer science wireless networks based on artificial intelligence, in 2012. He is currently working as an Associate Professor with the Faculty of Computers and Information, Minia University, Egypt. He is the Founder of the Computing & Artificial Intelligence Research Group (CAIRG), Egypt. He has more than 90 scientific research articles published in prestigious international journals in the topics of optimization, machine learning, image processing, and the IoT and its applications. His research interests include wireless sensor networks, the IoT, bioinformatics and biomedical, cloud computing, soft computing, image processing, artificial intelligence, data mining, optimization, and meta-heuristics techniques. He serves as a Reviewer of more than 30 journals, including Elsevier, Springer, and IEEE.